EFFECT OF SECONDARY THERMAL TREATMENT ON CRYSTALLINITY OF SPINEL-TYPE $Co(Cr,Al)_2O_4$ PIGMENTS SYNTHESIZED BY SOLUTION COMBUSTION ROUTE

Abstract

The effect of a post-synthesis thermal treatment on $CoCr_{2-2\Psi}Al_{2\Psi}O_4$ ($0.0 \leq \Psi \leq 1.0$) ceramic pigments synthesized by Solution Combustion Synthesis (SCS) has been studied. As-synthesized SCS pigments were treated at two different calcination temperatures (800 ºC and 1000 ºC) to study changes in mineralogy, microstructure and thermal behaviour, as well as their effect over the colouring power.

Spinel-type Fd-3m crystalline structure was developed in all cases. Nevertheless, crystallinity parameters were highly affected by both analysed processing parameters: composition (Ψ) and post-synthesis calcination temperature (T_c). A Cr(III) enrichment along with T_c increase favoured ion rearrangement to promote sample crystallization and crystallite growth. Fast kinetics of SCS makes Al-rich spinels with transition metals difficult to be synthesized. The application of a secondary thermal treatment resulted in a favourable evolution towards a well-crystallized structure. Lattice parameter did not seem to be affected by T_c, although it evolved indeed with composition. From a microstructural point of view, as-synthesized pigments were foamy, with a very low bulk density and nanometric grain size. After the thermal treatment, larger grain sizes were obtained, especially for the samples richer in Al and treated at higher T_c.

All pigments developed intense colours in a transparent glaze without showing heterogeneities, indicating a stable behaviour against glazing process. Glaze colour evolved from green to perfectly blue shades, indicating an important dependence on composition. Nevertheless, colouring power seemed to be rather affected by calcination process.

Highlights

- SCS allows synthesizing complex spinels with three cations (Co^{2+}, Cr^{3+}, Al^{3+})
- Composition and calcination temperature(Tc) modify crystal structure and grain size
- Calcination counteracts the negative effect of SCS kinetics on Al-spinel synthesis
- Regardless of the post-synthesis treatment, pigments showed high colouring power
- SCS pigments show thermal stability to manufacture inks for ceramic decoration

EFFECT OF SECONDARY THERMAL TREATMENT ON CRYSTALLINITY OF SPINEL-TYPE $Co(Cr,Al)_2O_4$ PIGMENTS SYNTHESIZED BY SOLUTION COMBUSTION ROUTE

J. Gilabert[a,*], M.P. Gómez-Tena[a], V. Sanz[b,c], S. Mestre[b,c]

[a]Instituto de Tecnología Cerámica. Asociación de Investigación de las Industrias Cerámicas. Castellón (Spain)

[b]Instituto Universitario de Tecnología Cerámica. Universitat Jaume I. Castellón (Spain)

[c]Departamento de Ingeniería Química. Universitat Jaume I. Castellón (Spain)

*Corresponding Author (jessica.gilabert@itc.uji.es)

Abstract

The effect of a post-synthesis thermal treatment on $CoCr_{2-2\Psi}Al_{2\Psi}O_4$ ($0.0 \leq \Psi \leq 1.0$) ceramic pigments synthesized by Solution Combustion Synthesis (SCS) has been studied. As-synthesized SCS pigments were treated at two different calcination temperatures (800 ºC and 1000 ºC) to study changes in mineralogy, microstructure and thermal behaviour, as well as their effect over the colouring power.

Spinel-type Fd-3m crystalline structure was developed in all cases. Nevertheless, crystallinity parameters were highly affected by both analysed processing parameters: composition (Ψ) and post-synthesis calcination temperature (T_c). A Cr(III) enrichment along with T_c increase favoured ion rearrangement to promote sample crystallization and crystallite growth. Fast kinetics of SCS makes Al-rich spinels with transition metals difficult to be synthesized. The application of a secondary thermal treatment resulted in a favourable evolution towards a well-crystallized structure. Lattice parameter did not seem to be affected by T_c, although it evolved indeed with composition. From a microstructural point of view, as-synthesized pigments were foamy, with a very low bulk density and nanometric grain

size. After the thermal treatment, larger grain sizes were obtained, especially for the samples richer in Al and treated at higher T_c.

All pigments developed intense colours in a transparent glaze without showing heterogeneities, indicating a stable behaviour against glazing process. Glaze colour evolved from green to perfectly blue shades, indicating an important dependence on composition. Nevertheless, colouring power seemed to be rather affected by calcination process.

Keywords: Combustion synthesis, pigment, spinels, crystallinity, microstructure

1 Introduction

Nowadays, the synthesis of oxidic materials with particle sizes in the nanometer and micrometer range, with the desired composition, purity, structure and specific properties for the targeted applications, has become one of the major challenges faced by material researchers and different industries as pigment manufacturers [1]. Solution combustion synthesis (SCS) is a novel technique used worldwide to obtain nanocrystalline oxide materials [2]. Currently, there are many methods to synthesize simple and mixed oxides: from the most traditional ones such as high temperature solid-state reaction (ceramic method) [3,4] or co-precipitation [5,6], to the most up-to-date wet-chemical ones such as the polymeric precursor technique [7,8] or sol-gel method [9,10], among others. All these techniques present important drawbacks as coarse product development, high temperature requirements, presence of impurities or difficulties in their processing, among others. SCS has been revealed as a breaking-down methodology to obtain oxide materials because of its simplicity, low energy demands and time-effectiveness [11]. The advantages of SCS are comprehensive at all processing levels: time and energy efficiency, simple equipment, less expensive raw materials than in other advanced methods, molecular mixing of components, and high purity and tuned composition of products [11].

SCS is a low-temperature-initiated self-propagated high-temperature combustion method [12-15]. It uses the highly exothermic reaction between oxidizers, typically metal nitrates, and organic fuels such as urea or glycine, to produce high temperature due to spontaneous combustion. The energy released by the reaction is used in the crystallization of the desired product. For that reason, SCS has emerged as a viable technique to prepare oxide materials for the ceramic sector such as pigments [16-18].

SCS has been reported to generate well-crystallized simple oxides and directly produce the desired final product. Despite all advantages that SCS process presents, little information is available on controlling SCS parameters [19] as the effects of fuel [20], initial solution concentration [21], flame [22-23] or calcination temperatures on product's characteristics. In fact, depending on the investigated system, a subsequent heat treatment of the synthesized powder (also called calcination process) is needed to promote the formation of the required phase and to avoid some secondary products like CO and NO_x that can appear because of the incomplete combustion process. Nevertheless, there is a lack of information about the effects of this step on the final properties of the oxide product. In fact, it has been reported that in SCS the phase, morphology, particle size and surface area of products can be altered to certain extents by adjusting combustion variables as calcination temperature, but it has to be studied for every specific case and product to be developed.

The present report is aimed at evaluating the effect that calcination temperature T_c exerts over the resulting properties (crystalline structure, crystallite size, grain size, specific surface area and particle agglomeration) of ceramic pigments $Co(Cr,Al)_2O_4$ developed by the Solution Combustion Synthesis, using urea as fuel. These properties depend heavily on the adopted processing parameters. Concretely, it is intended to define a well-structured template to obtain stable ceramic pigments, from a chemical and mineralogical point of view. It has been tried to go far beyond emphasizing the simple characterization of the synthesized materials, but to study in depth all changes undertaken in pigment characteristics when they

are calcined. Those data are necessary to evaluate the possible changes in pigment's colouring power when added to a glaze and fired.

Despite being two of the most important colour systems used in the ceramic industry [24], selected pigments $CoCr_2O_4$ and $CoAl_2O_4$ are not easily obtained as a well-crystallized product by the SCS method, as reported by some authors in previous works [25], especially, the Co-Al spinel. Thus, the fact of developing a new well-defined template combining SCS method with a short moderate-temperature secondary thermal treatment to get over the high temperature, time and energy-consuming of traditional ceramic method can be considered an important technological improvement for ceramic sector.

2 Experimental procedure

2.1 Materials and method

Solid solutions $CoCr_{2-2\Psi}Al_{2\Psi}O_4$ ($0.0 \leq \Psi \leq 1.0$, $\Delta\Psi = 0.2$) have been synthesized by solution combustion synthesis using water as solvent and urea as fuel. Solutions were prepared by mixing the corresponding metal nitrates (from Panreac Quimica) following their molar proportions (Table I) in 50 mL of distilled water with 24 g of urea as fuel.

The aqueous mixture was stirred in a 700-mL pyrex container during 30 min. and inserted in a preheated kiln at 500ºC (BLF 1800, Carbolite Furnaces Ltd, UK) for 20 min of soaking time to carry out the combustion process. Afterwards, the as-synthesized pigments were calcined at two different temperatures (800 ºC and 1000 ºC) for 1h in an electric furnace (RHF 1600, Carbolite Furnaces Ltd, UK). Each step followed to carry out SCS combustion is detailed in Fig. 1.

As-synthesized and calcined pigments were disaggregated in a ball mill with water as a fluid at 260 rpm for 15 min (Pulverisette 5, Fritsch GmbH, Germany). The suspensions were dried under infrared lights and the powder sieved through a 200-µm mesh.

Finally, 2/98 wt% pigment/frit glazes were prepared to evaluate colour development of samples. A transparent single-fired porous tile frit (chemical composition: 0.5% Na_2O 4.0 % K_2O, 15.3% CaO, 0.9 MgO, 9.0% ZnO, 7.4% Al_2O_3, 3.0% B_2O_3, 59.5% SiO_2) was selected to carry out the test. Glazed tiles were fired in an electric laboratory furnace using a single-fired floor tile thermal cycle at 1100ºC for 6 min of soaking time.

2.2 Pigments characterization

An X-ray diffractometer (Theta-Theta D8 Advance, Bruker, Germany), with CuK radiation (λ = 1.54183 Å) was used to characterize sample mineralogy and identify crystalline structures developed. The equipment generator applied an intensity light source of 45 kV and 40 mA. Diffraction data were analysed by means of a 2θ VÅNTEC-1 detector ranging from 5 to 90º (step width of 0.015º at 1.2 s/step). A refinement Rietveld protocol was performed using the specific software DIFFRACplus TOPAS (version 4.2). The agreement indices, as defined in Topas, for the final least-squares cycles of all refinements were in the following ranges: 1.23 ≤ Rwp (Weight profile R-factor) ≤ 2.53 and 1.14 ≤ GOF (Goodness of fit) ≤ 1.37.

A TGA-SDTA equipment (851E/160, Mettler Toledo, Switzerland) was selected to carry out thermal characterization by means of a simultaneous thermal analysis (ATD-TG) in a platinum vessel from 25 to 1000 ºC at 10ºC/min and using a dynamic air atmosphere (50 mL/min flow).

Microstructural characterization was performed with a FEG-SEM (QUANTA 200F, FEI Co, USA) and specific surface area was determined using a nitrogen volumetric equipment (Tristar 3000, Micromeritics, USA) by means of the BET (Brunauer-Emmet-Teller) theory. Samples were degassed at a temperature of 150ºC for 3 hour.

A spectrophotometer (Color Eye 7000A, X-Rite Inc, USA) was used to measure reflectance curves of the glazed tiles, and CIELab* chromatic coordinates were calculated using CIE Illuminant D65 and CIE 10º standard observer.

3 Results and discussion

Spongy samples were obtained in all cases (Fig. 1), being the most Cr-rich pigments the ones that occupied the highest volume of the container. Al-rich samples generated more compact products. The spongy masses showed no difficulties to disaggregate until obtaining a finely grained powder. Product's colours ranged from light greens, passing through dark green until obtaining intense blue shades.

3.1 Crystalline structure

In previous reports based on the same spinel-type composition [25-26] chemical analysis conducted on SCS samples showed a fairly good correlation between theoretical and experimental values of molar percentages of each solid solution conducted in the study. The results confirmed that pigment synthesis by SCS was developed in a very effective way. As a consequence, in the present report, no chemical data was analysed in order not to be redundant.

According to XRD results, and assuming chemical composition homogeneity, all synthesized pigments developed a well-defined face centered spinel-type structure, Fd-3m [27], independently of composition and T_c. Fig. 2 shows XRD analysis for as-synthesized samples as an example. The only crystalline phase identified has been labelled in their corresponding positions after identification. No additional crystalline phases were identified in the samples (reactants or secondary products), confirming the ion rearrangement into a spinel structure. Moreover, it was observed that the reflections ranged from the $CoCr_2O_4$ characteristic reflections to $CoAl_2O_4$ ones, according to published patterns [28-29].

Despite the similarities, diffraction patterns showed a significant evolution depending on composition and calcination temperature (Fig. 3). The effect of composition is considerable when comparing as-synthesized SCS pigments. Spinel main reflection evolves progressively from a well-defined peak at Ψ=0.0 to a practically amorphous hallo at Ψ=1.0. It means that as the composition enriched in Al(III) ion, crystallization of the spinel is hampered.

Conversely, Cr(III) ion favours the synthesis of high-crystallinity spinels. In consequence, Al(III) ion seemed to work against ion rearrangement into spinel-type structure.

Calcination process provoked an important improvement on sample's crystallinity. On one hand, this phenomenon is greater as the calcination temperature increases, because the most evident change is produced after the 1000 ºC treatment. On the other hand, the compositions richer in Al which generates the less crystalline products were the most sensible to the effect of calcination temperature. This fact means that SCS pigments can modify its crystallinity when added to a glaze and fired. In consequence, it can be thought that having a well-defined synthesis template, which combines SCS and a secondary thermal treatment, an optimization of pigment's structure can be achieved, obtaining better crystallized products with all ions occupying the suitable cell positions.

Crystallite size was calculated from Rietveld refinements carried out on diffraction patterns (Fig. 4). As expected, crystallite size of as-synthesized pigments experienced an important decrease from 80 nm to 5 nm as the composition becomes enriched in Al. However, the evolution was not linear. In fact, crystallite size showed a significant decrease in the chromium-rich spinels ($0.0 < \Psi < 0.2$), but the decreasing trend moderated progressively as the proportion of Al increased ($0.2 < \Psi < 0.8$), until practically stabilizing for the aluminium-rich spinels ($0.8 < \Psi \leq 1.0$). The effect of calcination was an increase of crystallite size in all samples, that was larger when lower crystallinity samples were treated and higher temperatures were employed. In fact, when composition favours crystallization ($\Psi=0.0$), small increases in the crystallite size were observed after calcination process. However, for $\Psi=1.0$ crystallite size increased practically ten times when treated al 1000 ºC, that is from 5 nm to 50 nm approximately. In addition, calcination effect was a function of T_c because the 800 ºC treatment increased crystallite size slightly in all the range of compositions. However, the 1000 ºC treatment provoked a significant increase in crystallite size, especially in the most Al-rich compositions.

Regarding lattice parameter behaviour (Fig. 5), a progressive decreasing was observed following the theoretical path stated by Vegard's law. It was consistent with the lower ionic radius of the Al(III) (0.39 Å) in comparison to the Cr(III) one (0.62 Å) in octahedral coordination. The lower the ion size, the shorter the distance between ions and, hence, a progressive decrease in the lattice parameter is produced [30].

Despite the general trend, experimental data seemed to experience a slight positive deviation from theoretical path. This behaviour was already observed by other authors [25,31,32], not giving clear explanation about the phenomenon responsible for the behaviour. On the other hand, no calcination temperature effect was observed in lattice parameter. In consequence, the SCS method directly generates the cubic cell corresponding to the initial composition, not a range of similar cells that reacts at high temperature to generate the expected one.

3.2 Thermal behaviour

The low crystallinity of the as-synthesized Al-rich samples and the important effects of the calcination treatment pointed to a complex thermal behaviour of this pigments. In consequence, thermal analyses were conducted on sample Ψ=1.0 after SCS combustion and after applying the calcination process at 1000 ºC to verify this point (Fig. 6). By the contrary, the as-synthesized Cr-rich pigments were well crystallized and were less modified by the calcination treatment, with low probability of showing thermally induced transitions.

As-synthesized sample showed three mass losses during the heating process, which were identified according to Hatakeyama et al. [33]. Firstly, a loss of water around 100ºC related to humidity and adsorbed water. Secondly, another loss of water at T≈400ºC, consequence of $Al(OH)_3$ decomposition. The last mass loss around 800 ºC was oxygen released by the Co_3O_4 to CoO reduction. All these events also appeared in the differential thermal analysis test, as observed at figure 6b. This thermal behaviour indicated that $CoAl_2O_4$ pigment obtained after SCS combustion was not perfectly synthesized. Not only the crystallite size was low, but some secondary low-crystallinity oxides, not detectable by XRD method, were present in the

sample. That secondary oxides become hydrated during the wet ball-milling. On the other hand, analysis of Ψ=1.0 sample obtained after calcination showed no thermal events, which indicates that all ions had rearranged in a suitable way and no unreacted oxides remained in the sample.

That facts reinforced the evidence that SCS presents some difficult to synthesize Al-rich spinels with transition metals [11], because of their fast kinetics that avoids a correct rearrangement of ions in a crystalline network. In consequence, in that cases secondary thermal treatments on spinel-type SCS pigments are desirable to complete the reaction and obtain a well crystallized structure free of secondary products.

3.3 Morphological characterization

The SEM analysis of selected samples demonstrated an evident influence of composition and calcination temperature over the microstructure (Fig. 7). A significant grain shape and size change was observed in as-synthesized pigments depending on composition. The structure of Ψ=0.0 pigment ($CoCr_2O_4$ spinel) consisted of partially-sintered round-shaped grains with a size around 100 nm. In the case of Ψ=0.4 pigment, well-sintered grains were obtained, which showed broader distributions in shape (some grains with angular shape) and size (from 50 nm to 200 nm), evidencing the effect of Al(III) on the composition. Finally, Ψ=1.0 pigments ($CoAl_2O_4$ spinel) presented very small grains (< 40 nm) with a characteristic "dry gel" microstructure, that was coherent with its low crystallinity.

After the calcination at 1000 ºC, pigment's microstructure showed important changes. In general, the grain size increases up to 200 – 300 nm interval, and the grain shape become more angular, although the changes in grain morphology were not homogeneous on the whole sample. Despite grain size growth, the crystalline habit of spinel was difficult to observe [34], although in some cases appeared in an incipient way.

In addition to SEM, specific surface area is considered a valuable parameter to evaluate microstructural changes in pigments. The SEM images visualizes changes in pigment's

microstructure which show a good correlation with specific surface area data obtained by BET method (table 2). These data give a quantitative measurement of the phenomena observed. In the case of as-synthesized pigments, the higher the grain size, the lower the specific surface area values obtained. This phenomenon was justified because bigger grains formed agglomerates with some big pores, but low porosity on the whole. By the contrary, when morphology consisted of very small grains (Ψ=1.0), the samples were sintered in a different way and resulted in microporous agglomerates, favouring the sharp increase in specific surface area [25]. However, specific surface did not show a clear trend in the case of calcined samples. The grain growth and the sintering process generated microstructures with bigger grain sizes and lower microporosities, with similar specific surfaces. The most pronounced change with calcination was found in the Ψ=1.0 pigment. Therefore, after applying a calcination process, it can be said that the negative effect of ion Al on the grain size development was made up. In fact, thermal treatment favoured their crystallization obtaining bigger grains with certain angled edges, a shape nearer to the crystalline habit of spinel.

3.4 Colouring power

Fired glazes showed intense colours and were free of surface defects (Fig. 8), which indicated that the pigments were stable against chemical attack by the molten glaze and that the decomposition reactions did not cause surface damage.

Developed colours ranged from green to blue tones as the composition enriched in Al. Reflectance curves of glazes (Fig. 9) showed the evolution of colour versus composition and calcination temperature. The evolution of reflectance spectra can be interpreted taking in account the interaction between the individual reflectance spectra of Co and Cr ions [35]. Cr(III) absorbs nearly all visible spectra except the interval correspondent to green ($450 \leq \lambda \leq 550$ nm), and Co(II) reflectance bands lies in the blue zone ($\lambda \leq 450$ nm). In addition, the two ions have reflection bands in the infrared whose tail reaches the visible range. Therefore, absorption band of chromium overlapped the reflectance band of cobalt which nearly only

lefts the red tail when Co and Cr proportions are adequate, as it happens at Ψ=0.8. On the other hand, Al(III) has no absorption in the visible range and only affects the reflectance spectra slightly modifying the energy levels of cobalt ion and, thus, its emission and absorption spectra. T_c effect over reflectance curves was low, as it slightly displaces some intervals of the curves to lower values of reflectance, except for the Ψ=1.0 pigments case, where the curve was displaced to higher values.

CieLab* coordinates show practically no variation of colour depending on calcination temperature, as expected from the reflectance curves (Fig. 10). L* and a* components practically showed no variations (Fig. 10 a). Only b* coordinate (Fig. 10 b) seemed to be somewhat influenced by this temperature, since samples calcined at 1000 ºC generated glazes with a higher blue component when there was some Cr(III) in the composition than in the rest of the cases.

Regarding composition effect, Al enrichment favoured obtaining darker, less greener and less bluer colour tones. However, the total substitution of chromium produced pigments which provoked a sudden change in glaze's colours, which were lighter than the corresponding to the Ψ=0.8 ones, with red shade and the highest blue component. This last case corresponds with the cobalt blue spinel.

Colour development seemed to maintain a definite dependence with composition. Post-synthesis thermal treatments, however, can only modulate colouring power but they do not change the general trend. Only b* coordinate is more sensitive to T_C, as blue component increases appreciably in some cases when the 1000 ºC treatment was applied ($0.2 \leq \Psi \leq 0.8$). The low effect observed over colour, regardless calcination temperature, is due to the fact that during the firing of glazed tiles, carried out at 1100ºC, pigments evolved to a better-crystallized structure with bigger grain size, at least until the glaze begins to melt and interact with the pigments. In consequence, the state of the pigments can be quite close to that of the treated ones at 1000 °C. An additional investigation would be necessary to

determine the T_C values that would correspond to the end of the heating section of the firing of the glaze for each composition.

4 Conclusions

Solution Combustion Synthesis allowed synthesizing very fluffy pigments consisting of solid solutions of spinels $CoCr_{2-2\Psi}Al_{2\Psi}O_4$ ($0 \leq \Psi \leq 1$ in steps of 0.2) being Cr-rich ones the spongiest. The ions present in the solutions rearranged in a spinel-type Fd-3m structure, although aluminium-rich samples contained some non-integrated aluminium oxides, which were highly reactive with water. Pigment composition influences crystallite size, lattice parameter and grain size. In addition, calcination allows crystallite and grain size to increase with respect to the as-synthesized ones, favouring ion rearrangement of crystalline network and working against the negative effect of SCS fast kinetics.

Regarding microstructure, the grain size decreased and specific surface increased as Al content increased in the as-synthesized pigments, but not in a regular trend. After calcination, the grains become more angular and bigger, but the size increment was a function of composition and calcination temperature.

All pigments presented intense colours, with a high colouring power when added to the transparent glaze, without generating defects, implying thermal and chemical stability. Composition affected colour development since Cr-rich pigments allowed obtaining higher green shades while Al-rich pigments developed intense blue glazes. Calcination effect was only noticeable in blue component, as pigments calcined at higher temperatures generated more intense blue shades, except for the pure $CoAl_2O_4$ pigment.

It has been demonstrated that SCS spinel-type pigments colouring power is stable enough despite post-synthesis thermal treatments. Nevertheless, other crystalline and microstructural characteristics can be modified. In consequence, they could be used to manufacture inks for ceramic decorations without additional thermal treatments to stabilize the crystalline structure.

Acknowledgements

The authors thank Universitat Jaume I for their support for the development of this research (Project Nr. P11B2015-04).

Bibliography

[1] S. T. Aruna, *Solution Combustion Synthesis-An Overview*, 206-221, *Combustion Synthesis: Novel routes to novel materials*. M. Lackner (Ed.), Viena University of Technology, Austria (2010).

[2] W. Wen, J.M. Wu, "Nanomaterials via solution combustion synthesis: a step nearer to controllability," *RSC Adv.* 4 (2014) 58090-58100. doi: 10.1039/c4ra10145f

[3] P. Escribano, J.B. Carda, E. Cordoncillo, "Esmaltes y pigmentos cerámicos", Enciclopedia cerámica, Faenza Editrice Ibérica, Castellón, 2001

[4] J.M. Rincón, J. Carda, J. Alarcón, Nuevos productos y tecnologías de esmaltes y pigmentos cerámicos: su fabricación y utilización, 1ª ed., Faenza Editrice Ibérica-Sociedad Española de. Cerámica y Vidrio, Castellón (España), 1992

[5] I.V. Pishch, E.V. Radion, "A pigment based on coprecipitated iron (III) and nickel (III) hydroxides," *Glass Ceram.*, 53 (1996) 178–179. doi:10.1007/BF01166033

[6] I.V. Pishch, E.V. Radion, "Use of the precipitation method in the synthesis of ceramic pigments," *Glass Ceram.*, 62 (2005) 189-191. doi:10.1007/s10717-005-0069-2

[7] L. Gama, M. A. Ribeiro, B.S. Barros, R.H.A. Kiminami, I.T. Weber, A.C.F.M. Costa, "Synthesis and characterization of the $NiAl_2O_4$, $CoAl_2O_4$ and $ZnAl_2O_4$ spinels by the polymeric precursors method," J. Alloy Compd. 483 (2009) 453-455. doi:10.1016/j.jallcom.2008.08.111

[8] L.K.C. de Souza, J.R. Zamian, G.N. da Rocha, L.E.B. Soledade, I.M.G. dos Santos et al. "Blue pigments based on $Co_xZn_{1-x}Al_2O_4$ spinels synthesized by the polymeric precursor method," Dyes Pigments 81 (2009) 187–192. doi:10.1016/j.dyepig.2008.09.017

[9] P. Escribano, M. Marchala, M. L. Sanjuán, P. Alonso-Gutiérrez, B. Julián, E. Cordoncillo, "Low-temperature synthesis of SrAl2O4 by a modified sol–gel route: XRD and Raman characterization," J. of Solid State Chem. 178 (2005) 1978–1987. doi:10.1016/j.jssc.2005.04.001

[10] S. Sanjabi, A. Obeydavi, "Synthesis and characterization of nanocrystalline $MgAl_2O_4$ spinel via modified sol–gel method," J. Alloy Compd. 645 (2015) 535–540. doi:10.1016/j.jallcom.2015.05.107

[11] K.C. Patil, M.S. Hedge, T. Rattan, S.T. Aruna, "Chemistry of nanocrystalline oxide materials: Combustion synthesis, properties and applications," World Scientific Publishing, Singapore, 2008.

[12] J.J. Kingsley, K.C. Patil, "A novel combustion process for the synthesis of fine particle α-alumina and related oxide materials," Mater. Lett. 6 (1988) 427-432. doi:10.1016/0167-577X(88)90045-6

[13] S.T. Aruna, K.C. Patil, "Synthesis and properties of nanosized titania," J. Mater. Synth. Proces. 4 (1996) 175-176. S.T. Aruna, K.C. Patil, "Synthesis and properties of nanosize titania," J. Mater. Synth. Processing 4 (1996) 175-179.

[14] M.A. Rodríguez, C.L. Aguilar, M.A. Aghayan, "Solution combustion synthesis and sintering behaviour of $CaAl_2O_4$," Ceram. Int. 38 (2012) 395-399.

[15] K. Suresh, K.C. Patil, "A combustion process for the instant synthesis of α -Fe_2O_3," J. Mat. Sci. Lett. 12 (1993) 572-574. doi:10.1007/BF00278328.

[16] R. Ianoş, A. Tăculescu, C. Păcurariu, I. Lazău, "Solution combustion synthesis and characterization of magnetite, Fe_3O_4, nanopowders," J. Am. Ceram. Soc. 95 (2012) 2236-2240. doi: 10.1111/j.1551-2916.2012.05159.x

[17] S.S. Manoharan, K.C. Patil, "Combustion synthesis of metal chromite powders," J. Am. Ceram. Soc. 75 (1992) 1012-15. doi: 10.1111/j.1151-2916.1992.tb04177.x

[18] A.C.F.M. Costa, A.M.D. Leite, H.S. Ferreira, R.H.G.A. Kiminami, S. Cava, L. Gama, "Brown pigment of the nanopowder spinel ferrite prepared by combustion reaction," J. Eur. Ceram. Soc. 28 (2008) 2033-2037. doi:10.1016/j.jeurceramsoc.2007.12.039

[19] A. Alves, C.P. Bergmann, F.A. Bellutti, Novel Synthesis and characterization of nanostructured materials, Chapt. 2: Combustion Synthesis, Springer-Verlag Berlin Heidelberg, 2013. doi: 10.1007/978-3-642-41275-2

[20] D.P. Tarragó, C. de Fraga Malfatti, V.C. de Sousa, "Influence of fuel on morphology of LSM powders obtained by solution combustion synthesis," Powder Technol. 269 (2015) 481-487, doi: 10.1016/j.powtec.2014.09.037

[21] J. Gilabert, M.D. Palacios, V. Sanz, S. Mestre, "Solution combustion synthesis of (Co,Ni)Cr_2O_4 pigments: Influence of initial solution concentration," Ceram. Int. 43 (13) (2017) 10032-10040. IN PRESS. doi: 10.1016/j.ceramint.2017.05.019

[22] M. C. Gardey Merino, A. L. Estrella, M. E. Rodriguez, L. Acuña, M. S. Lassa, G. E. Lascalea, P. Vázquez, "Combustion syntheses of $CoAl_2O_4$ powders using different fuels," Proc. Mat. Sci. 8 (2015) 519 – 525. doi: 10.1016/j.mspro.2015.04.104

[23] A.S. Mukasyan, P. Epstein, P. Dinka, "Solution combustion synthesis of nanomaterials," P. Combust. Inst. 31 (2007) 1789–1795. doi:10.1016/j.proci.2006.07.052

[24] Color Pigments Manufacturers Association (CPMA), Classification and chemical descriptions of the complex inorganic color pigments, fourth ed., Alexandria (VA), 2013.

[25] J. Gilabert, M.D. Palacios, V. Sanz, S. Mestre, "Fuel effect on solution combustion synthesis of Co$(Cr,Al)_2O_4$ pigments," Bol. Soc. Esp. Ceram.V. 56 (2017) 215-225. doi: 10.1016/j.bsecv.2017.03.003

[26] J. Gilabert, M.D. Palacios, V. Sanz, S. Mestre, "Characteristics reproducibility of (Fe,Co)$(Cr,Al)_2O_4$ pigments obtained by solution combustion synthesis," Ceram. Int. 42 (2016) 12880-12887. doi:10.1016/j.ceramint.2016.05.054

[27] K.E. Sickafus, J.M. Wills, "Structure of spinel," J. Am. Ceram. Soc. 82(1999) 3279–3292. doi: 10.1111/j.1151-2916.1999.tb02241.x

[28] International Center for Diffraction Data (ICDD) PDF-4+ file, ICDD 04-014-1636.

[29] International Center for Diffraction Data (ICDD) PDF-4+ file, ICDD 04-008-3316.

[30] D.R. Lide (Ed), CRC handbook of chemistry and physics, 74th ed, CRC Press, Boca Raton, 1993.

[31] I.C. Nlebedim, J.E. Snyder, A.J. Moses and D.C. Jiles, "Effect of deviation from stoichiometric composition on structural and magnetic properties of cobalt ferrite, $Co_xFe_{3x}O_4$ (x=0.2 to 1.0)," J. Appl. Phys. 111 (2012) 07D704. doi: 10.1063/1.3670982

[32] J. Shou-Yong, L.Z. Jin, L. Yong, "Investigation on lattice constants of Mg-Al spinels," J. Mat. Sci, Lett. 19 (2000) 225-227. doi: 10.1023/A:1006710808718

[33] T. Hatakeyama, L. Zhenhai (eds.) Handbook of thermal analysis. Reimp. Chichester: John Wiley & sons, 2000.

[34] F. J. Torres, E. Ruiz de Sola, J. Alarcon, "Effect of some additives on the development of spinel-based glass-ceramic glazes for floor-tiles," J. of Non-Cryst. Solids 351 (2005) 2453–2461. doi: 10.1016/j.jnoncrysol.2005.06.027

[35] J.M., Fernández Navarro, El vidrio: constitución, fabricación, propiedades. Madrid: Instituto de Cerámica y Vidrio, 1985.

Figure captions

Figure 1 Scheme of lab sequence followed to obtain SCS pigments, calcination and colour development

Figure 2 XRD phase identification for all composition range of $CoCr_{2-2\Psi}Al_{2\Psi}O_4$ ($0 \leq \Psi \leq 1$) samples as-synthesized (● spinel)

Figure 3 Diffraction patterns around I_{100} of the synthesized pigments $CoCr_{2-2\Psi}Al_{2\Psi}O_4$ ($0.0 \leq \Psi \leq 1.0$) versus Ψ, calcination temperature and kiln atmosphere

Figure 4 Evolution of spinel crystallite size depending on parameter Ψ and calcination temperature

Figure 5 Comparison of lattice parameters of the spinel with the prediction of Vegard's law, based on the ICCD data from the spinels $CoCr_2O_4$ (Ψ = 0.0) and $CoAl_2O_4$ (Ψ = 1.0)

Figure 6 Simultaneous thermal analyses of samples Ψ=1.0, as-synthesized and after calcination at 1000 ºC: a) Thermogravimetric analyses, b) Differential thermal analyses

Figure 7 Micrographies obtained by SEM of synthesized pigments

Figure 8 Example of glazed samples with as-synthesized pigments, showing saturated colours with no defects on the surface

Figure 9 Reflectance curves of the glazes that contain the synthesized pigments

Figure 10 Evolution of chromatic coordinates of glazes versus composition and thermal history of the incorporated pigment: a) L* and a*coordinates and b) b* coordinate

Tables and table captions

Table 1 Initial solution composition for each synthesized spinel

Ref.	Ψ	$Co(NO_3)_2 \cdot 6H_2O$ (g)	$Cr(NO_3)_3 \cdot 9H_2O$ (g)	$Al(NO_3)_3 \cdot 9H_2O$ (g)
S1	0.0	17.46	48.01	---
S2	0.2	17.46	38.41	9.00
S3	0.4	17.46	28.81	18.00
S4	0.6	17.46	19.21	27.01
S5	0.8	17.46	9.60	36.01
S6	1.0	17.46	---	45.01

Table 2 Specific surface area values (m^2/g) for selected samples

Composition	Treatment	
	As-synthesized	T_c = 1000 ºC
Ψ=0.0	13	24
Ψ=0.4	29	9.7
Ψ=1.0	226	8.4

Figure 1
Click here to download high resolution image

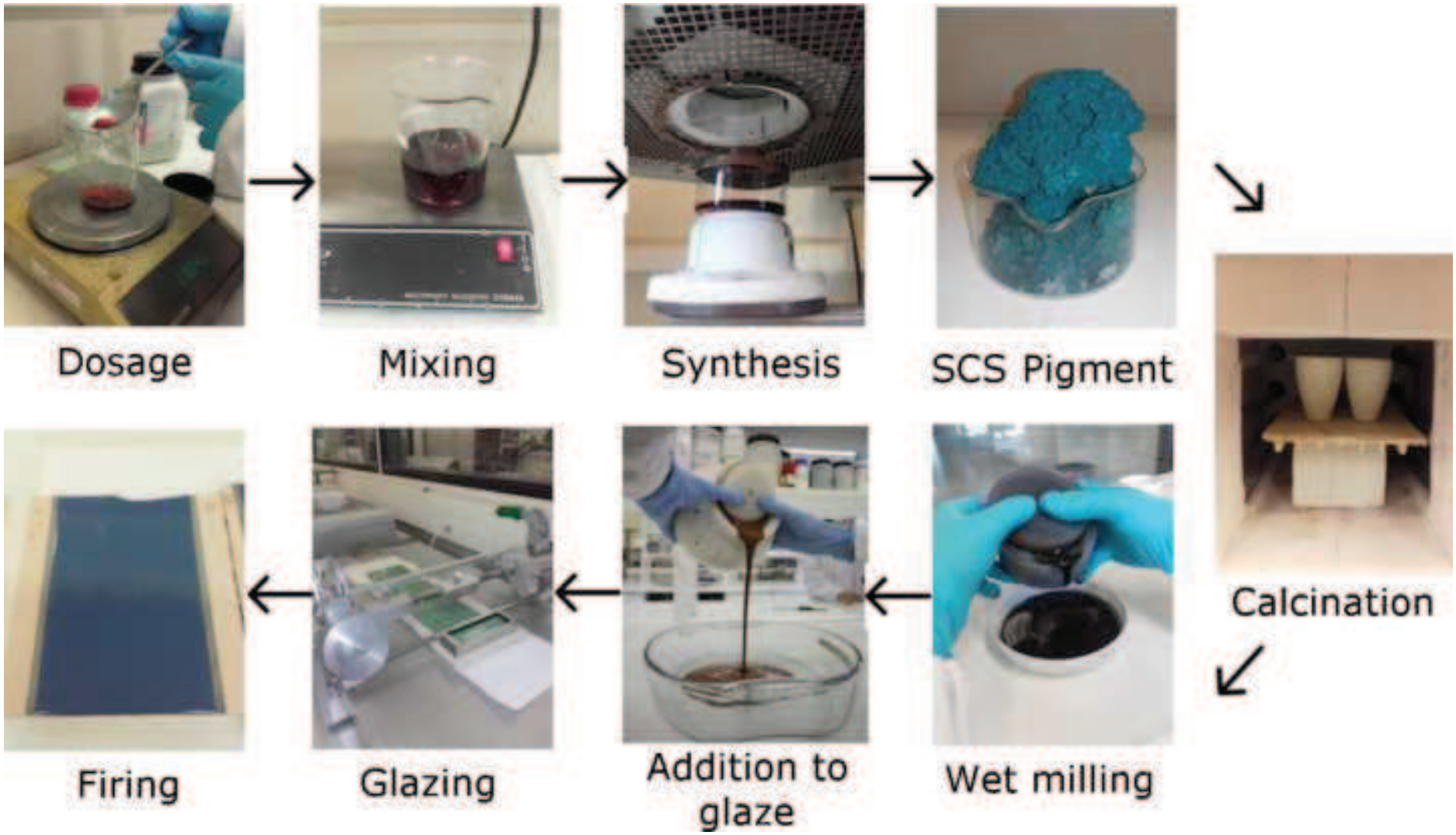

Figure 2
Click here to download high resolution image

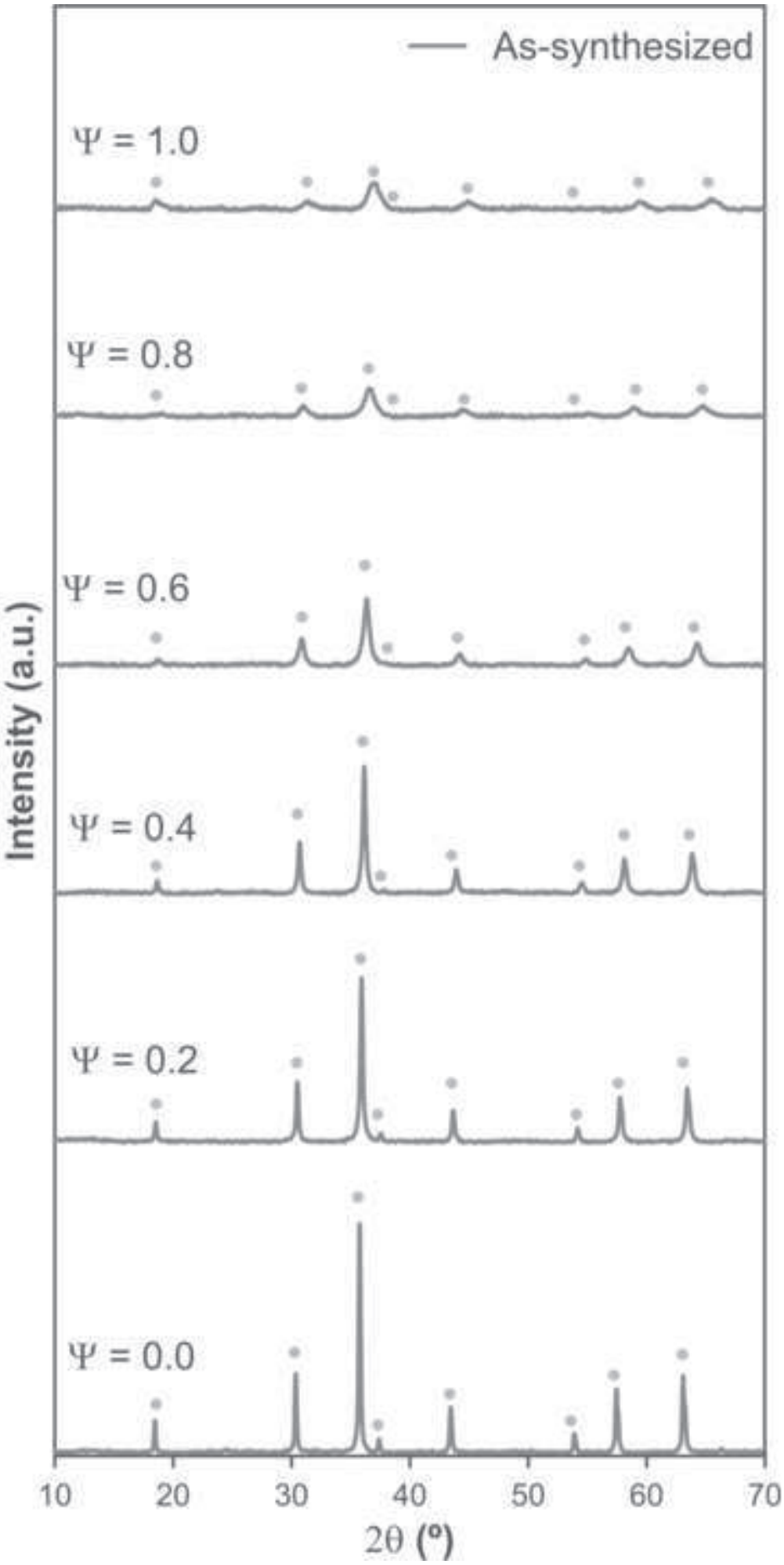

Figure 3
Click here to download high resolution image

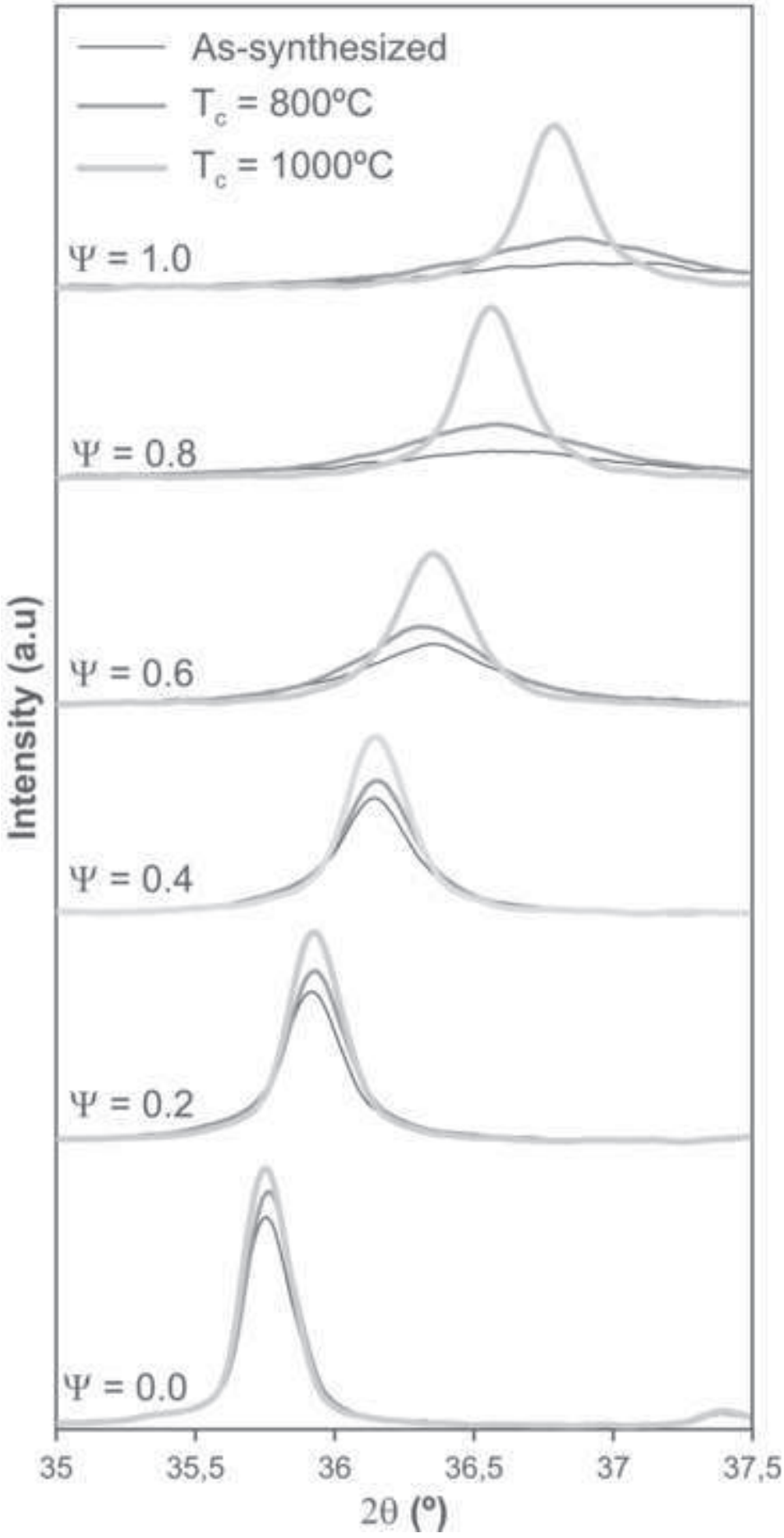

Figure 4
Click here to download high resolution image

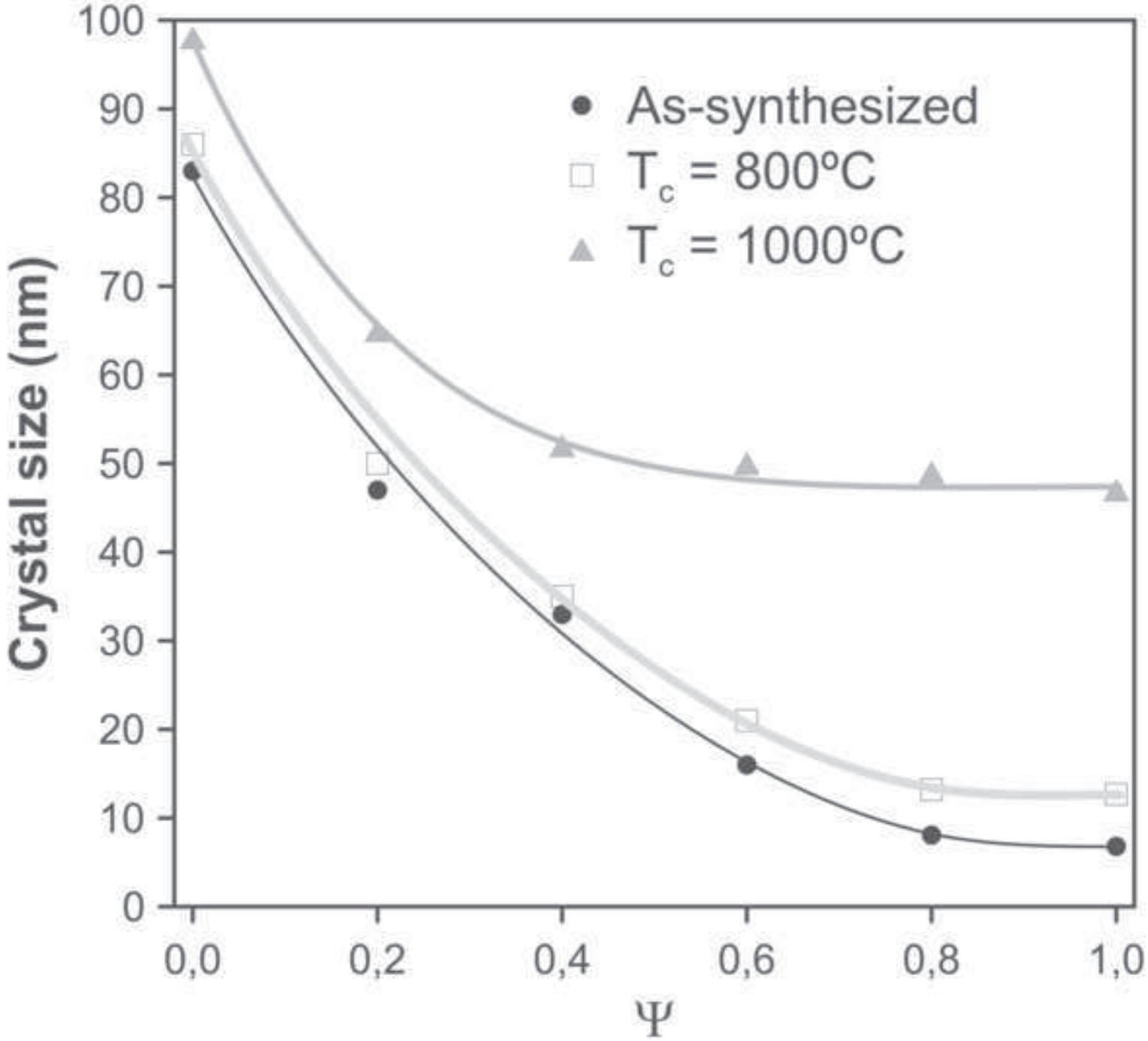

Figure 5

Click here to download high resolution image

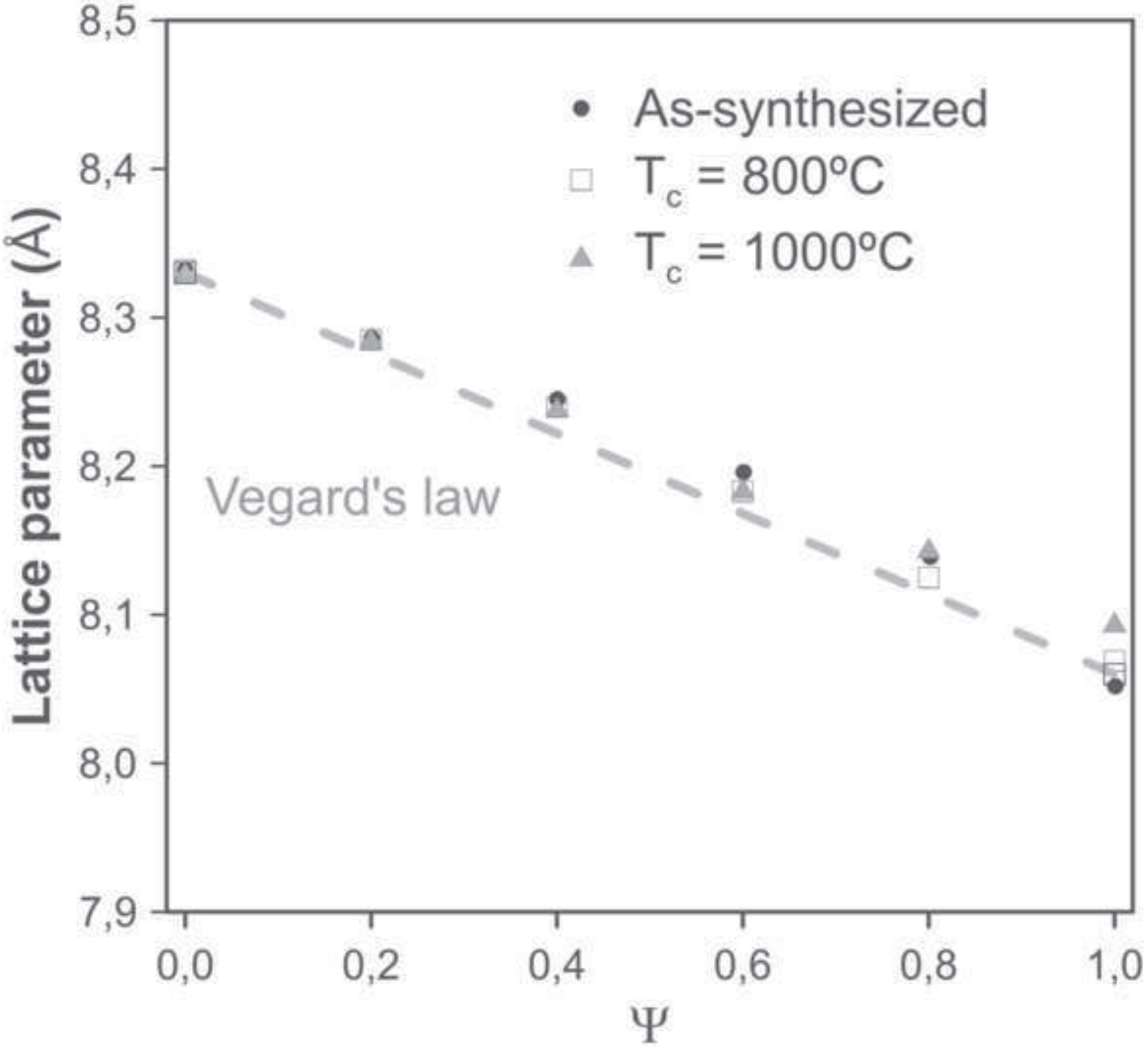

Figure 6
Click here to download high resolution image

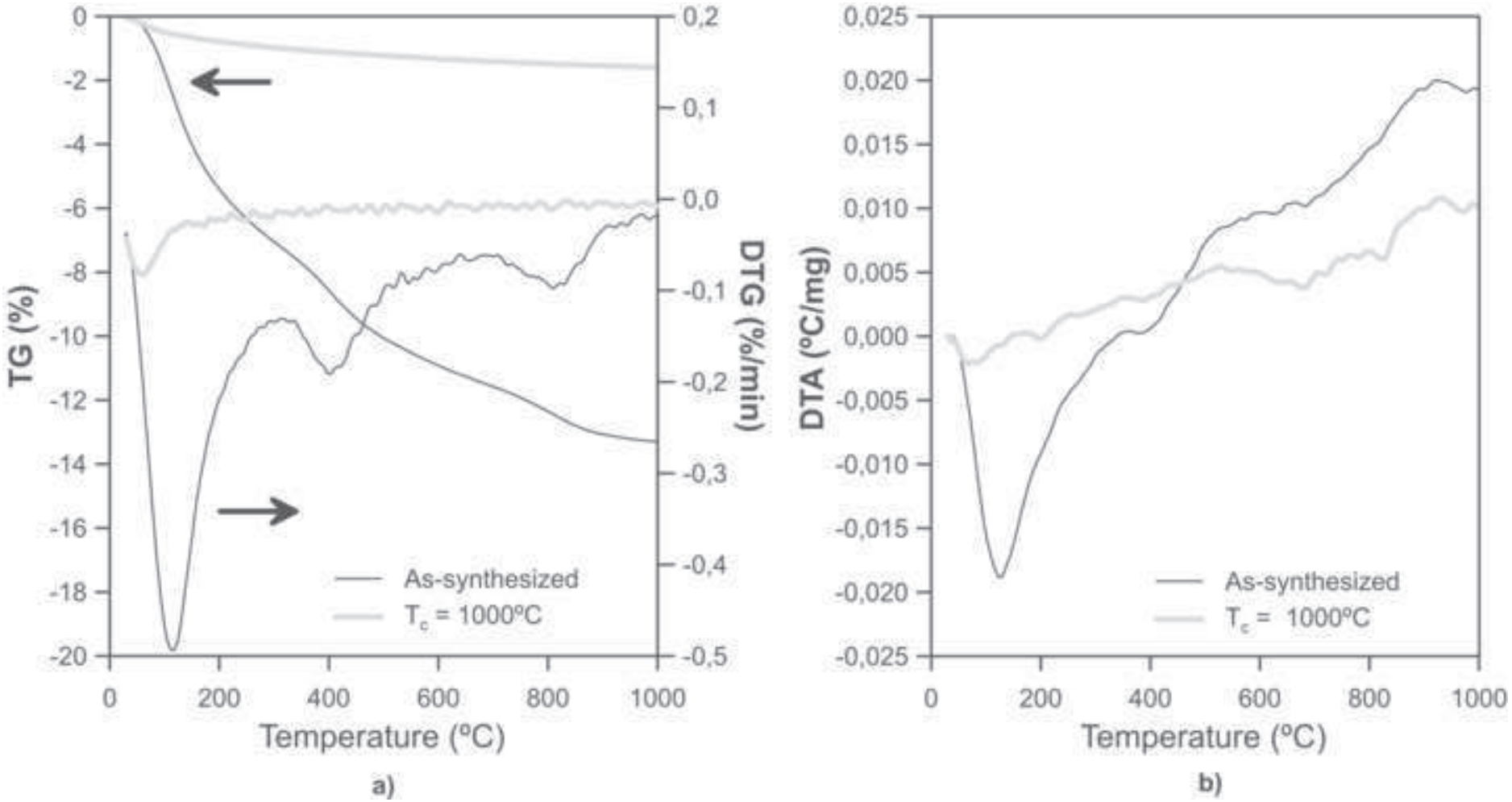

Figure 7
Click here to download high resolution image

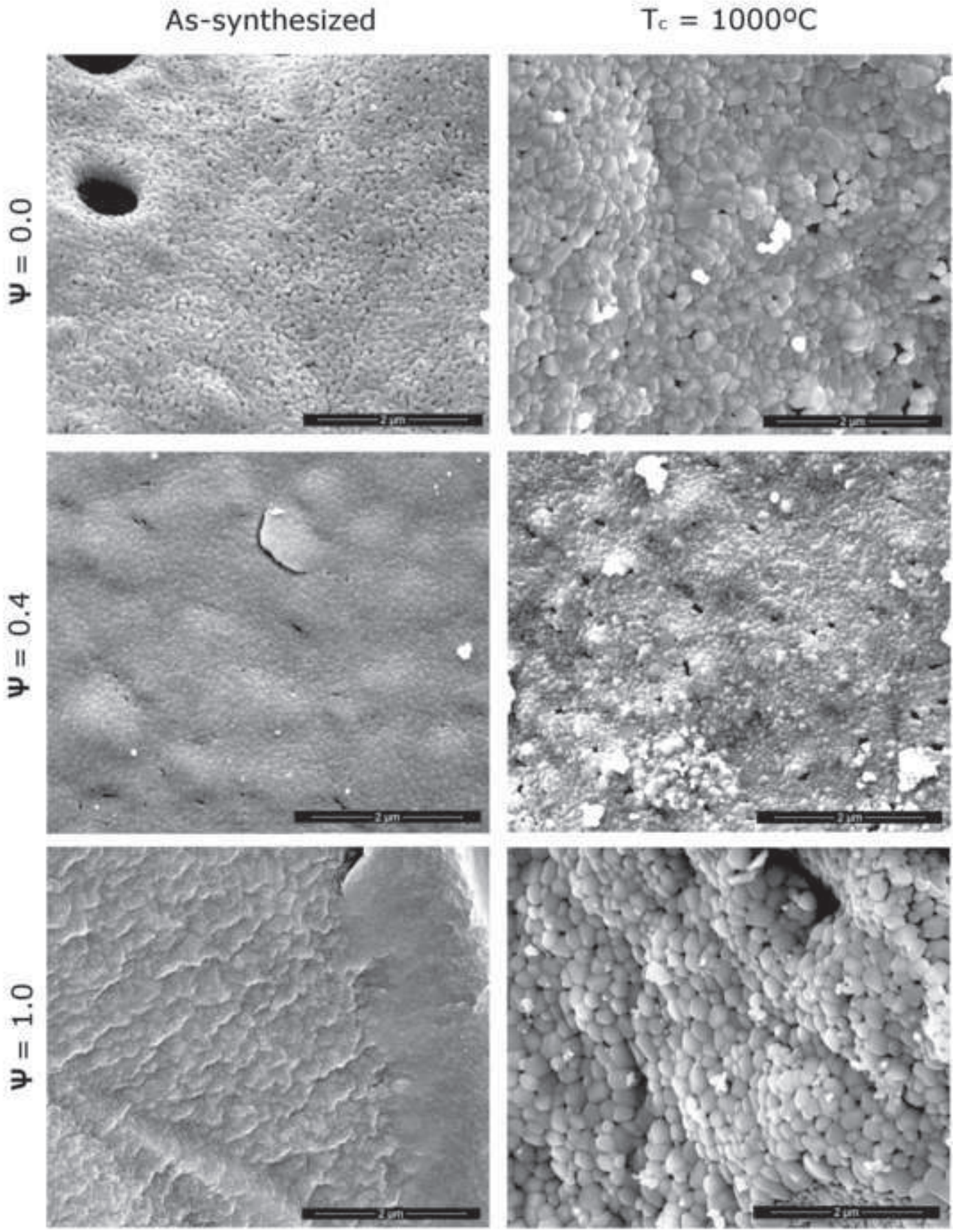

Figure 8
Click here to download high resolution image

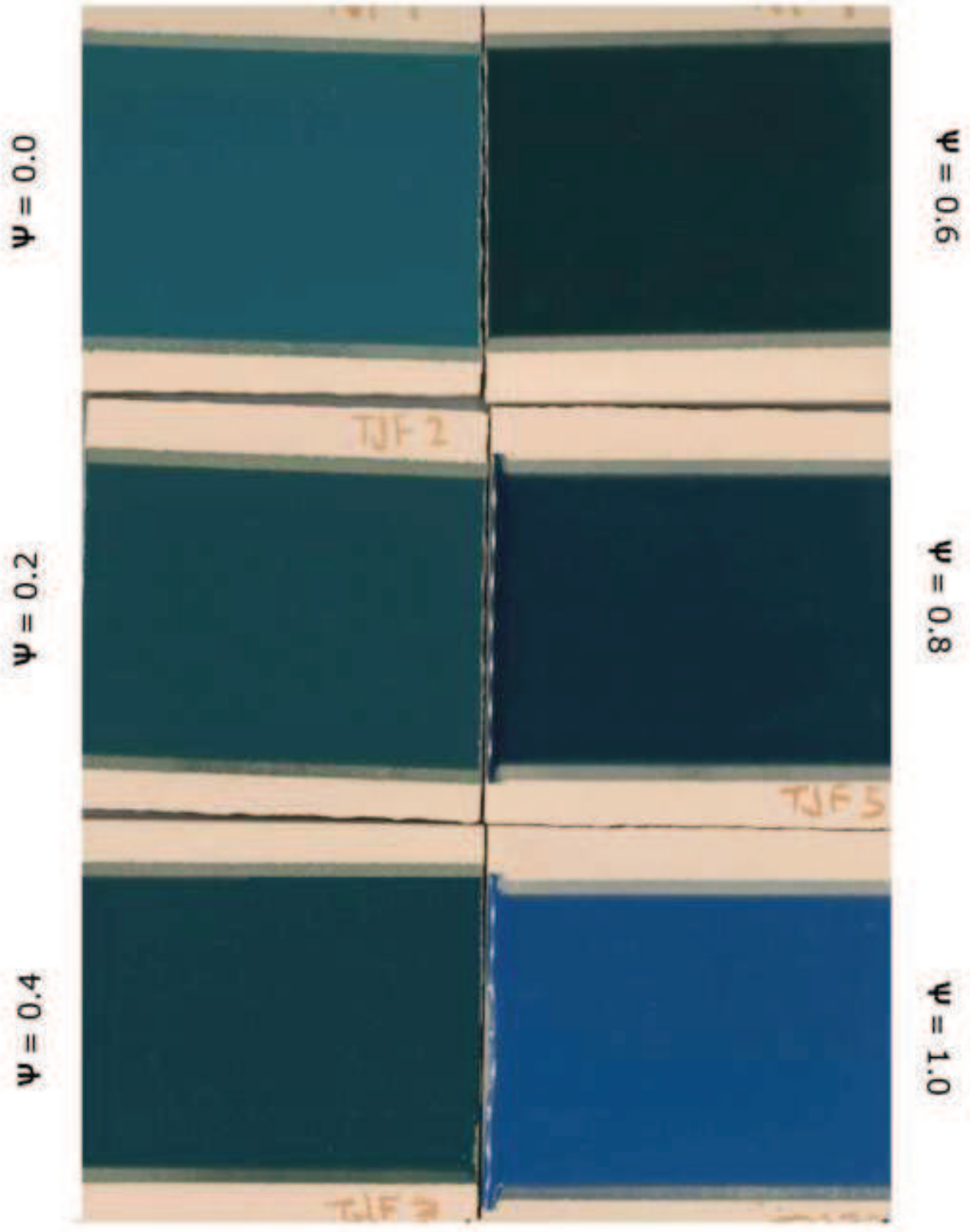

Figure 9
Click here to download high resolution image

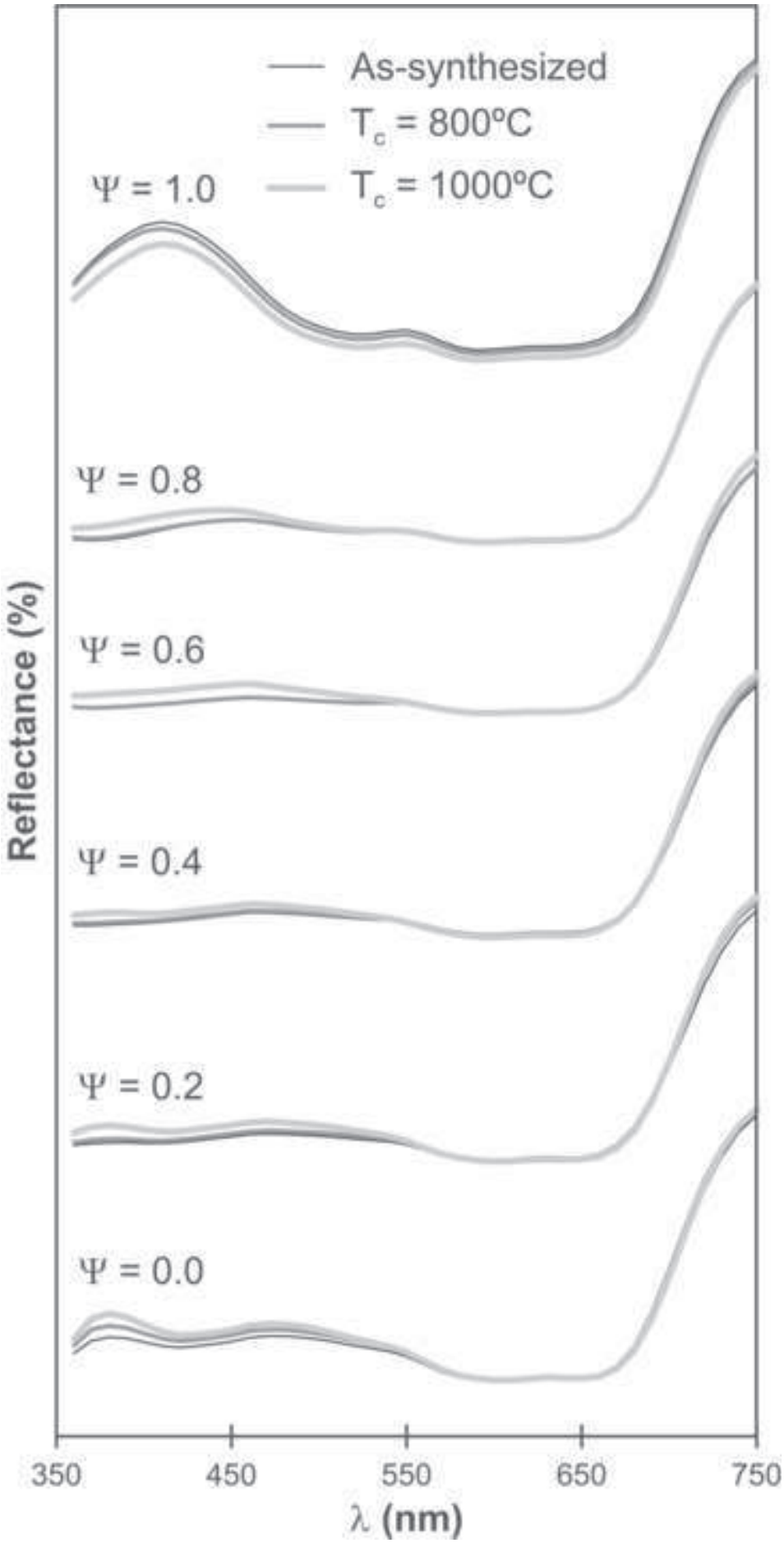

Figure 10
Click here to download high resolution image